A00-16300

AIAA-2000-0401

TOWARDS HYBRID LES-RANS COMPUTATIONS OF CAVITY FLOWFIELDS

S. Arunajatesan and N. Sinha
Combustion Research and Flow Technology, Inc. (CRAFT Tech)
Dublin, PA 18917

and

S. Menon
Georgia Institute of Technology
Atlanta, GA 30332

38th Aerospace Sciences Meeting & Exhibit
10-13 January 2000 / Reno, NV

TOWARDS HYBRID LES-RANS COMPUTATIONS OF CAVITY FLOWFIELDS*

S. Arunajatesan†, and N. Sinha††
Combustion Research and Flow Technology, Inc.
Dublin, PA 18917
sinha@nas.nasa.gov
and
S. Menon‡
Georgia Institute of Technology
Atlanta, GA

ABSTRACT

Development of a hybrid approach that attempts to merge LES and RANS methodologies with a view to solving practical problems is explored. The one equation LES model [6,9] and a length scale RANS model [7,13,16] are examined. A priori testing of the LES model using DNS data for isotropic turbulence shows that the LES model correlates very well with the DNS. Examination of the RANS model shows that in order to merge the two models, a variable grid dependent coefficient has to be used. Using this coefficient is seen to mimic the behavior of the eddy viscosity as obtained from a filtered DNS flowfield. The correlations with the subgrid eddy viscosity at fine resolution limits show that the LES model behavior is recovered in the fine mesh limit.

INTRODUCTION

Currently, a computational research initiative to study the flowfield around an aircraft weapons bay is underway. The overall goal of this effort is directed towards attenuation of dynamic loads in a weapons bay and developing a strategy to achieve controlled release of stores from aircraft, taking into account the highly turbulent and unsteady environment surrounding the bay. In order to achieve this goal, a full understanding of the flowfield surrounding the bay must first be obtained. The weapons bay flowfield is very strongly affected by many characteristics such as the flight velocity, the bay geometric features, the presence of stores in the bay, the upstream boundary layer etc. Moreover, a wide variety of physical phenomena, e.g. highly unsteady vortex shedding, and strong pressure oscillations characterize this flow[1]. Hence, in order to accurately model the weapons bay flowfield and its effect on the stores released from the bay, a detailed model that can capture all the features affecting the flow field and resolve all the fluid dynamic phenomena must be used.

The computational techniques presently available to model these flows can be categorized as Direct Numerical Simulations (DNS), Large Eddy Simulations (LES) and Reynolds Averaged Navier-Stokes Simulations(RANS). DNS attempts to simulate the entire range of time and length scales present in the flow. The length and time scales in the cavity flow range from small scale boundary layer flow upstream of the cavity, to the large scale vortices shedding off the leading edge of the cavity, to the large recirculation bubble encompassing the bay. Simulating this entire range of scales completely in a DNS is infeasible at this point Therefore, turbulent modeling techniques (LES and RANS) have to be resorted to in order to simulate the weapons bay flowfield.

RANS methodology attempts to model the effect of the entire range of turbulent scales while simulating only the mean flow field. These methods work well for steady flows, or, at best, unsteady flows with very weak non-resonant coupling. These models are inadequate for flows that are highly unsteady and involve strong vortex-acoustic coupling and resonance like phenomena. In the LES methodology, cognizance is taken of the fact that on any given computational mesh, a certain range of scales can be accurately resolved and only the scales that are not resolved need to be modeled. Hence, in this method, only the large energy containing scales (i.e., scales that are inhomogeneous and boundary condition dependent) are computed directly, while the effects of the more universal small scales, are modeled. Because of this, the methodology is capable of handling the flows for which RANS models work and also for flows involving strong vortex-acoustic coupling, resonating pressure disturbances. However, this added advantage of the LES method comes at the expense of computational cost. LES methods are typically an order of magnitude more expensive than their RANS counterparts.

Hence, while RANS methods are deficient in their ability to predict flows that are well suited for LES methods, using LES methods to simulate flows that RANS methods can predict is overkill. The cavity flowfield, however, comprises embedded regions that require LES methods (like the shear layer over the cavity, the near field upstream boundary layer, and the flowfield surrounding the store) surrounded by regions where RANS methods may be adequate (like the far upstream boundary layer and the rest of aircraft etc.). Therefore, using any one method for the entire flowfield is bound to, either, yield wrong results (if RANS methods are used) or, prove to be too expensive (if LES methods are used). Therefore, a hybrid method that combines these two

*AIAA-2000-0219, 38th AIAA, Aerospace Sciences Meeting and Exhibit, Reno, NV, Jan 10-13, 2000.
† Research Scientist, Member AIAA.
†† Vice-President and Technical Director, Associate Fellow AIAA.
‡ Professor, Senior Member, AIAA.

approaches will be very useful in modeling the weapons bay flowfield.

Despite this apparent usefulness of a hybrid LES-RANS method, relatively little effort has been devoted to the development of such a method. To the best of the authors knowledge, the work by Speziale[2] is the only published work relating to such approaches. In his paper, Speziale proposes a method in which the Reynolds stresses and subgrid scale(SGS) stresses are computed through a model of the form

$$\tau_{ij} = \left[1 - exp\left(-\beta\Delta / L_k\right)\right]^n \tau_{ij}^{(R)} \qquad (1)$$

where $\tau_{ij}^{(R)}$ is the Reynolds stress tensor, Δ is the local mesh width, L_k is the Kolmogorov length scale, and β and n are modeling constants. If the mesh is highly resolved, $\Delta/L_k \to 0$, all relevant scales are resolved, and equation (1) approaches a direct simulation where $\tau_{ij} = 0$. At the other limit, as $\Delta/L_k \to \infty$ and the mesh becomes coarse or the Reynolds number (based on cell width Δ) becomes large, a Reynolds stress model is recovered. In order to model the Reynolds stress tensor, Speziale recommends the use of an two equation RANS model augmented to include non-equilibrium effects through an explicit algebraic stress model. While this might yield a more accurate description of the Reynolds stress tensor, the behavior of the hybrid model as per equation (1) is strongly dependent on the coefficients β and n. Evaluation of the modeling constants are not discussed in that paper. However, in defining his approach to hybrid VLES-RANS method, Speziale has defined a few criteria that such an approach must satisfy in order to be consistent and physically correct. These serve as a valuable guide to anyone attempting to develop a hybrid approach and are discussed below.

The criteria outlined by Speziale can be enumerated as follows:

a) Use of any test filters or double-filtered fields that can contaminate the large scales of motion must be avoided;
b) A systematically derived anisotropic eddy-viscosity that is strain dependent and allows for the direct integration of the SGS models to solid boundaries must be incorporated; and,
c) A state of the art Reynolds stress model must be recovered in the coarse mesh limit.

The need for the third criterion is obvious. Any simulation should yield meaningful results at all points in the computation and should not need to be tuned for different flows/meshes. The model should, depending on the flow and the mesh used, naturally transition from the LES regime in the fine resolution regions to the RANS regime in the coarse resolution region. The first criterion is necessary because, in practical computations, the exact filter is never known. Further, inversion of filtered quantities results in a Fredholm integral equation of the first kind[2], which is mathematically ill-posed. Thus it is necessary to avoid the use of test filtered quantities since accurate de-filtering can never be accomplished.

However, the need for the second criterion is not as clear. In his paper, Speziale recommends using Explicit Algebraic Stress Models (EASM) to model the Reynolds stress tensor in equation (1). These models are derived by invoking the equilibrium assumption and hence the net effect reduces to the imposition of strain dependence on the eddy viscosity. However, the effect of these corrections to the basic k-ε model has been observed to be slight[3]. Moreover, it has been noted by researchers in the past (see for example, reference [4]) that, the deficiencies in using the resolved scale strain rates to model unresolved turbulence stems from the misalignment of the two tensors. That the imposition of a strain rate dependence on the scalar eddy viscosity significantly alters the deficiency is not clear. Further, in the LES limit, the turbulence that is being modeled is in the inertial/dissipation range and the behavior of these models in this limit is not clear. Therefore, it is not clear at this point that this recommendation is absolutely necessary.

In light of the above discussion, we have adopted a slightly different approach to this problem. The starting point in Speziale's approach was the RANS model. He attempted to improve the model for non-equilibrium flows and then proposed a method of extending it to the fine resolution or LES limit. Here, we start with an LES model and examine RANS models with a view to coupling it with the LES model. We explore the feasibility of computing a turbulent length scale directly to enable the natural transition of the turbulence model from LES to the RANS limit. To this end, we have studied the behavior of the turbulent length scale based on the two point single time correlations tensor obtained from a DNS simulation. In the following sections we outline the basic approach adopted. The baseline LES model and the RANS models are discussed. A priori testing of the LES model using the DNS data is presented to verify the model quality. Then, we present a summary of results from an LES calculation of a model weapons bay geometry using the one equation model to show that the basic LES approach works well for this problem. This is also out motivation for developing a hybrid approach which will reduce to the LES model in the fine resolution limit. Finally, we present an analysis of the hybrid approach using data from the DNS of isotropic turbulence.

Basic Approach

Since the goal of this effort is to build a hybrid model that combines LES and RANS approaches into one unified approach, it is instructive to look at the overall modeling philosophy adopted in these two schools. In both LES and RANS, the averaging procedure (filtering in LES and ensemble averaging in RANS) results in unclosed "turbulent stress" terms in the governing equations. Borrowing from the kinetic theory expression for laminar viscous stresses in Newtonian fluids, these stresses are modeled as being proportional to the product of the local strain rates and an "eddy viscosity" (ν_T). The

expression for this eddy-viscosity is derived from dimensional arguments and takes the form

$$\nu_T = u' l \qquad (2)$$

where u' is a turbulent velocity scale and l is a turbulent length scale. The various models differ in their definitions for the velocity and length scales.

In LES, the length scale is defined by the filter width and is known a priori. It is also common to all the models. The differences in LES models arise in the definition of the velocity scale. For example, the Smagorinsky model[5] expresses the velocity scale as $u' = \Delta(2\bar{S}_{ij}\bar{S}_{ij})^{1/2}$ (where $\bar{S}_{ij}$ is the filtered strain rate), the one equation model[6,9] defines the velocity scale in terms of the kinetic energy as $u' = k^{1/2}$.

In the RANS limit, however, a length scale that characterizes turbulence is required and hence a second variable is required. The k-ε model of Launder and Spalding [18], the k-ω models of Wilcox [19] and the k-kl model proposed by Mellor and Herring [13] are examples of turbulence models that solve for two turbulence variables. All the three models solve a transport equation for the turbulent kinetic energy. This turbulent kinetic energy is then used to define a velocity scale for the turbulence. They differ in their definitions for the turbulent length scale. While the first two models express the length scale in terms of the dissipation rate ($l = k^{3/2}/\varepsilon$) and vorticity ($l = k^{1/2}/\omega$) respectively, the k-kl model solves a transport equation for the length scale of turbulence directly.

Thus, all turbulence models attempt to estimate the turbulence that is modeled through a velocity and length scale estimate. Amongst the RANS models, the solution of the kinetic energy seems to be a consensus method to estimate the velocity scale, while modeling the length scale seems to be the primary source of differences between the models. In LES models, on the other hand, the length scale is fixed by the mesh while the velocity scale estimates differ from model to model. However, the one equation model offers a possible way to bridge the gap between the LES and RANS approaches. If a length scale can be identified that goes, in the fine resolution limit, to the LES filter width and, in the coarse resolution limit, goes to the length scale computed from a state of the art RANS model, this length scale can be used to define the eddy viscosity. Such a model will naturally transition from being an LES model in the regions of fine resolution to an RANS model in regions of coarse resolution.

The above criterion defines LES as the natural starting point because this defines one known limiting value for the length scale. Hence, in our present approach we start from the one equation LES model and attempt to explore the RANS models to develop a hybrid approach. Although the k-ε model is by far the most popular of the RANS models, in this paper, we restrict our attention to the k-kl RANS model. This model represents a more direct approach to developing the hybrid model through a bridging of the length scales than the k-ε or the k-ω models. Also, the equation for kl used in this model is physically more realistic, has a better wall behavior and is numerically more robust than the dissipate rate equation for the k-ε model[7]. Also, the model equation for the dissipation rate used in the k-ε model is representative of a length scale that characterizes the energy containing scales rather than the small scales. The kl equation on the other hand is based on an integral of the two point correlation function and is more realistic at small scales.

The procedure we have used to evaluate the hybrid approach is as follows. A direct simulation of homogeneous isotropic turbulence is carried out. Using numerical filters (only the box filter, which is used in the LES calculations, is used here), this data is filtered down to coarser levels. First, this filtered flow field is used to evaluate the LES model performance. Then, the length scale model is studied. Its behavior in the fine resolution limit is compared with that of the LES model. Special attention is paid to the eddy-viscosity predicted by the two models.

Direct Numerical Simulations

As mentioned above, a DNS flowfield is generated in order to analyze candidate models for the hybrid approach. For this purpose, we simulate isotropic turbulence in a periodic box. The experiment of Comte-Bellot and Corrsin [8] is used for this purpose. In that experiment, grid generated turbulence behind two meshes, of one and two inch mesh spacing respectively, were studied. Detailed measurements of the velocity fluctuations, energy and dissipation spectra and velocity correlations were made at three locations downstream of the mesh, where the turbulence is decaying and isotropic. Numerically, this is simulated as decaying isotropic turbulence in a periodic box. This represents a box of turbulence convecting with the mean flow and the spatial evolution of the turbulence in the experimental setup is equivalent to the temporal evolution of the turbulence in the simulation. The size of the box is chosen to be much greater than the integral length scale of the turbulence. The energy spectrum at the first experimental location is used to initialize the simulations and comparisons are made at the two downstream locations.

In the experiment, the mesh size was two inches, the mean velocity was 10 m/s and the Reynolds number based on the mesh spacing and mean flow was 34000. The measurement locations correspond to non-dimensional times $t_{CBC} = 42, 98, 171$, where t_{CBC} is given by

$$t_{CBC} = \int_0^x \frac{d\xi}{U(\xi)} \qquad (3)$$

where, x is the downstream distance from the mesh and U(x) is the mean velocity.

In the numerical simulations, the cube dimension was taken to be 43.787 cms. This is much larger than the turbulent length scales (including the velocity integral length scale and the length scale corresponding to the peak in the energy spectrum). The initial conditions for the

velocity field were chosen to match the experimental spectrum and were generated in a manner identical to that described in the literature [12,17]. The initial conditions for pressure was obtained by solving the poisson equation. The initial temperature field was assumed uniform. In the results presented here, time is non-dimensionalized by 0.1secs for convenience.

The numerical scheme employed to simulate the isotropic turbulent flow is a variant of the fourth order MacCormack scheme developed by Nelson [9]. It was shown[9] that this scheme yields true fourth order accuracy and is also less dissipative than the original fourth order scheme proposed by Turkel et al. [10].

The DNS was conducted on a 128^3 uniform mesh. Ghosal et al.[11] estimated the resolution required to simulate this flow and concluded that in order to resolve 99.8% of the spectrum, a 512^3 grid would be required. They also estimated that on a 128^3 grid, only 92.2% of the energy will be resolved. Hence, in the initial spectrum, all the energy above the maximum wave number possible on the current grid was set to zero before the velocity field was computed.

Before proceeding to use the DNS results to analyze the LES and RANS models, the DNS spectra and resolved kinetic energy evolution is compared with experiment to ensure its accuracy. Figure 1 shows the comparison of the decay of turbulent kinetic energy with the experimental data from [8]. The three experimental points denote the three locations at which measurements were made – DNS results were saved only from a non-dimensional time of 0.1. However, the initial field was chosen to match the experimental spectrum. Clearly, the evolution is captured accurately.

Figure 2 shows the evolution of the turbulent kinetic energy spectrum. Comparison with the experimentally measured spectra at the two downstream locations is shown – the agreement between the computed and experimental profiles is excellent. Thus we now have an accurately simulated isotropic flow field that can be used to study the turbulence models.

The LES Model

The one equation LES model solves for a transport equation for the subgrid kinetic energy. This is then used to evaluate the eddy viscosity that is used to model the unresolved SGS stresses. The model equations are as follows

$$\frac{\partial \bar{\rho}\tilde{k}}{\partial t}+\frac{\partial}{\partial x_i}\left(\bar{\rho}\tilde{u}_i\tilde{k}-\bar{\rho}\nu_T\frac{\partial \tilde{k}}{\partial x_i}\right)=\tau_{ij}^{sgs}\frac{\partial \tilde{u}_i}{\partial x_j}-D_k \qquad (4)$$

where, k is the Favre filtered subgrid kinetic energy, $\tilde{u}_i$ is the resolved scale velocity, $\bar{\rho}$ is the filtered density, $\tau_{ij}^{sgs}=\bar{\rho}(u_iu_j-\tilde{u}_i\tilde{u}_j)$ is the subgrid scale tensor, ν_T is the subgrid scale eddy viscosity and D_k is the dissipation of the SGS kinetic energy. The subgrid scale stresses are modeled as

$$\tau_{ij}^{sgs}=-2\bar{\rho}\nu_T(\tilde{S}_{ij}-\frac{1}{3}\delta_{ij}\tilde{S}_{kk})+\frac{2}{3}\bar{\rho}\tilde{k}\delta_{ij} \qquad (5)$$

The eddy viscosity is computed as

$$\nu_T=C_\nu\tilde{k}^{1/2}\Delta \qquad (6)$$

where, C_ν is the modeling constant. It has been computed to be equal to 0.0667[9]. This constant has been recomputed here using the DNS results. We now present a discussion of the model behavior using the DNS simulations.

Testing of the LES Model

In order to do this, we have used the conventional method used by other researchers in the past[4,12]. Using the DNS results, the "exact" turbulent stresses on any grid coarser than the DNS grid can be computed. From the filtered velocity field, the model turbulent stresses are then computed, which can then be compared to the "exact" stresses to yield a measure of the quality of the model. Since the SGS stress is actually a tensor quantity, this comparison can be made at various levels. At the tensor level, each individual component of the stress tensor is compared. At the vector level, the acceleration term $\frac{\partial \tau_{ij}^{sgs}}{\partial x_j}$ appearing in the momentum equation is compared to the exact acceleration term computed directly from the DNS field. At the scalar level, the energy dissipation term appearing in the energy equation $\frac{\partial u_i\tau_{ij}}{\partial x_j}$ is compared. The comparisons are made in a statistical sense, the correlation coefficient between the "exact" terms and the modeled terms is used as a measure of the model quality. For any exact quantity E modeled using M, this is given by

$$C_{E-M}=\frac{<M.E>}{<M^2>^{1/2}<E^2>^{1/2}} \qquad (7)$$

where the angled brackets denote averaging over the whole domain. This measure is independent of the constants used in the model. The model coefficient is evaluated by equating the rms values of the exact and modeled stresses (the terms appearing in the denominator of equation (7)). The scalar level constant, however, is traditionally used as the most appropriate value [4,12] for the model.

At the tensor level, differences are to be expected in the correlations for the diagonal and off diagonal terms – the correlations are averaged over the diagonal terms and the off-diagonal terms and are presented here separately. For the vector level, the correlations are averaged over all the components.

Tensor Level

Mesh	Correlation		Constant ($x10^2$)	
	D	OD	D	OD
32^3	0.38316	0.4219	9.002	7.4752
48^3	0.40139	0.42836	7.1261	6.2613
64^3	0.42499	0.44134	6.0992	6.6565
96^3	0.49914	0.4805	6.0018	4.9638

Vector Level

32^3	0.37913	6.0667
48^3	0.39364	5.8916
64^3	0.42136	6.1263
96^3	0.43801	5.4816

Scalar Level

32^3	0.48163	6.0137
48^3	0.5014	5.8937
64^3	0.5257	5.4013
96^3	0.57149	5.9185

Table 1. Correlation coefficients and model coefficients evaluated at various grid levels for the one equation LES model.

We have carried out the above exercise on 4 grid levels – 96^3, 64^3, 48^3, 32^3. The correlation coefficients for these grids at the tensor, vector and scalar levels are given in Table 1. First of all, the correlations at all the levels are reasonably good – the correlations in all the three levels (scalar, vector and tensor) are in general seen to improve as the grid resolution is increased. Further, the correlations at the scalar level are seen to be higher for all the resolutions than at the tensor or vector levels. These trends are all consistent with the trends seen in other researchers' works[4,12].

The model constant for all the cases presented here is seen to lie around the same range. Even when the resolution is varied by a factor of 3 in each direction the variation in the constants is seen to be less than 10%. A slight decrease in the constants is seen from the tensor to the vector to the scalar levels, however, in all the cases the agreement with the value of 0.0667 evaluated by other workers [6,9] for this model is very good. Thus it is concluded that the LES model is very reliable and performs well for the flow chosen. Other modeling assumptions and the models for other term, such as those appearing in the energy equations can also be studied using this method. However, in this paper we restrict ourselves to the momentum equation stress tensor. Analyses of the other terms will be presented in a future report. We now present a summary of results from a pulsed blowing study of weapons bay flows conducted using this model to demonstrate the model performance for such flowfields.

LES of Weapons Bay Flows

The model bay under consideration is a simple rectangular cavity of L/D=6. The flow Mach number is 1.47 and the Reynolds number is 7 million per foot. In the pulsed blowing cases, mass injection is carried out from a slot jet of 0.1in. at the leading edge of the cavity. Four cases are considered – the baseline case with no blowing, a steady blowing case, and two pulsed blowing cases, one with the jet pulsed at 100Hz and the second at 300Hz. In all the cases shown here, the mass blowing rate for the pulsing (or steady blowing) is 0.5lbm/sec.

Case	Fore End SPL (dB)	Aft End SPL (dB)
Baseline	182.44	186.69
Steady Blowing	170.66	183.41
Pulsed (100Hz)	177.13	187.28
Pulsed (300Hz)	170.78	178.88

Table 2. Results from LES of model weapons bay dynamic loads for the four cases considered are listed at the fore and aft bulkheads of the cavity.

Table 2 shows the dynamic loads measured in the cavity on the fore and aft bulkheads for the four cases. In all the cases shown, the dynamic loads are substantially higher on the aft end than on the fore end. Visualizations of the cavity flow field showed that this is due to the impingement of the vortices from the cavity shear layer on the aft corner. The boundary layer upstream of the cavity separates and forms a shear layer. The growth of instabilities in the shear layer leads to vortex shedding. These vortices convect downstream and impinge on the aft corner, giving rise to a large increase in the dynamic load on the aft bulkhead.

The spectra of the sound pressure levels (SPL) at the mid-point of aft bulkhead of the cavity is shown in figure 3. For the baseline case, a dominant mode of about 480 Hz is observed. With steady blowing for this case, a large suppression of the dynamic loads at the fore end is seen while the suppression is less than 3dB for the aft end case. The ffts reveal that at the aft end, the dominant mode is just shifted to a slightly higher frequency, without much suppression. When the jet is pulsed at 100 Hz (the frequency for this case is chosen arbitrarily), while the overall dynamic load decreases at the fore end, the dynamic load at the aft end is actually increased. A look at the SPL spectra reveals that the most dominant mode has actually been amplified from about 175 dB to 182 dB. A third jet blowing case was also studied. Since the noise level is related to the impingement of vortices at the aft end of the cavity, it was hypothesized that disrupting the shedding of these vortices must reduce the load on the aft end of the cavity. A look at the spectrum for the fore end suggested that the vortex roll-up occurs at a frequency of around 300Hz. Hence, for the fourth case, the jet was pulsed at 300Hz. It can be seen that in this case substantial suppression of the dynamic load is seen at the fore and aft

ends – 12dB at the fore end and 8dB at the aft end. A look at the SPL spectra reveals that the most dominant mode along with all the low frequency modes are completely suppressed. A single peak at around 1500Hz (too high a frequency to be of concern with respect to structural loading) is the only dominant mode observed. Thus the strategy of disrupting the leading edge vortex shedding is seen to be effective in achieving suppression.

While highlighting a possible method for noise suppression through low frequency pulsing, the above results also highlight a drawback of this technique. While low frequency pulsing offers an effective way to target certain frequencies, it often results in frequency shifting, whereby, instead of damping the overall energy level, it merely enables shifting of the dominant energy level in the flow to a different frequency. Hence, currently, other methods for noise suppression are being explored and results from these calculations will be detailed in a future report. The primary goal of this section is to demonstrate that this flowfield can be reliably simulated using the one equation LES model. Hence, we now proceed to examine the *k-kl* model and the hybrid approach.

The k-kl Model

The *k-kl* model was first proposed by Mellor and Herring[13]. The idea to model a length scale of turbulence was first put forth by Kolmogorov [14] and Rotta [15]was actually the first one to derive this equation. Rotta (and later Wolfshtein[16]) started with the equation for the two point correlation tensor $R_{ij} = \langle u_i(\mathbf{x}) u_j(\mathbf{x}+\mathbf{r}) \rangle$, and by first contracting this equation and then averaging and integrating over a sphere of radius r, derived an equation for the product of the length scale and the turbulent kinetic energy. This equation is given by

$$\frac{\partial \bar{\rho}\tilde{k}l}{\partial t} + \frac{\partial}{\partial x_i}\left(\bar{\rho}\tilde{u}_i\tilde{k}l\right) = \left(\bar{\rho}C_1 k^{1/2} l \frac{\partial \tilde{k}l}{\partial x_i} + \bar{\rho}C_1 k^{3/2} l \frac{\partial l}{\partial x_i}\right) + P_{kl} - D_{kl} \tag{8}$$

In fact, Mellor and Herring [13], showed that a general equation for $k^{(n/2)}l^m$ can be derived in a similar manner – the form of the equation is the same with differences only in the diffusion term. The basic premise of all such models is the same – they all attempt to express the eddy viscosity as

$$\nu_T = C_\nu^* \tilde{k}^{1/2} l \tag{9}$$

Thus, whichever form is used, of relevance is the behavior of the length scale itself and therefore, in our analysis, we look at the behavior of the length scale and the eddy viscosity obtained from using this length scale only. The actual form of the transport equation and the other modeled terms is left for later considerations. To this end, we define the length scale as follows (this is the same definition used by others [13,16])

$$kl(\mathrm{x}) = \frac{3}{16}\int_{-\infty}^{\infty} R_{ii}(\mathrm{x}, r)dr \tag{10}$$

and the eddy viscosity is computed from equation (9).

From the above definition it is apparent that this length scale, on LES grids, can be computed in two ways. In the first method, *kl* computed on the DNS field is filtered down to coarser levels like any other variable (say, velocity) and l is computed from $l' = kl/\tilde{k}$. In the second method, *kl* is computed from the correlations on the filtered velocity field directly using equation (10). Length scales computed through both these methods showed very similar quantitative and qualitative behavior and hence only the first method is used here since it is easier to use the same algorithm used to obtain filtered velocity fields to obtain the filtered length scales. However, the similarity in the length scales obtained in the two ways allows us to understand the behavior of the length scale in terms of the filtered velocity field, which is easier to visualize.

At this point it must be stressed that the quantity for which a model is being sought for is the eddy viscosity. While the possibility of finding a length scale that over the entire range (from LES to RANS) will yield the correct eddy viscosity (based on correlations with the "exact" stresses from a DNS, say) is very attractive indeed, it is overly simplistic to expect that this is possible. Therefore, it will be instructive to understand the behavior of the eddy viscosity itself before proceeding to look at the length scales.

In order to do this we define the following

$$\nu_s = \frac{\tau_{ij}^{sgs,exact} - \frac{2}{3}\bar{\rho}\tilde{k}\delta_{ij}}{-2\bar{\rho}(\tilde{S}_{ij} - \frac{1}{3}\delta_{ij}\tilde{S}_{kk})} \tag{11}$$

ν_s is the ratio of the "exact" turbulent stresses to the strain rate terms appearing in the model of equation (5). This represents the eddy viscosity that needs to be modeled. Using only the positively correlated terms, figure 4 shows a plot of the distribution of ν_s for various grid resolutions. This shows the expected trend, the distribution of the eddy viscosity shifts towards the smaller values for finer grids indicating that any model should attempt to dissipate a smaller fraction of the energy as the grid is refined. The coarseness of the PDF at the 8^3 grid level shows that the numerator and denominator in the right hand side of equation (11) have opposite signs at a fairly large number of points. This highlights the basic deficiency of this class of models – the misalignment of the turbulent stress tensor and the resolved scale strain tensor.

From this figure the expected behavior of the terms on the right hand side of equation (9) is now known. From the energy spectrum it is clear that as the grid becomes coarser, the magnitude of unresolved kinetic

energy increases. This is because a larger part of the spectrum lies beyond the cut-off wave number. The behavior of the entire right hand side term of equation (10) will be determined by the behavior of the length scale (equation (10)).

The behavior of the length scale is in turn determined by that of the correlation function. Fortunately, the behavior of R_{ii} is well understood (at least in homogeneous isotropic turbulence). $R_{ii}(x,r)$ is unity for $r=0$. For $r > 0$, R_{ii} decreases with increasing r. For any flow, R_{ii} becomes zero for all $r>r_c$, i.e., the velocity field becomes uncorrelated beyond a certain critical distance. Now consider the DNS flowfield. When this is filtered down to coarser and coarser levels, the points on the coarse mesh are moving farther apart, and therefore becoming less correlated with each other. Hence, for all meshes coarser than the DNS mesh, the correlation R_{ii} will decrease with increasing mesh spacing and hence the integral in equation (10) will decrease. Therefore, the product kl will decrease on coarser meshes. Since we know that k increases with increasing mesh spacing, it is clear that the behavior of kl is dominated by the behavior of l itself. Further, it can be concluded that if kl decreases, $k^{1/2}l$ is bound to decrease with increasing mesh spacing. Therefore, an eddy-viscosity based on equation (9) will decrease with increasing mesh spacing

It must be noted here that this is likely not a shortcoming of the kl model alone. Mellor and Herring [13] show that the k-kl model, k-ε model and the k-ω model can all be derived from each other with very slight differences in their forms. Hence, it is more than likely that a length scale computed from any of these models will behave in a similar fashion.

From the above discussion it is clear that the model coefficient C_v^* must no longer be a constant. It must vary with grid resolution in order to compensate for the behavior of the length scale. Using the DNS data the value of the coefficient can be computed. Again, similar to the method used for the LES, the coefficient is computed at the tensor, vector and scalar levels. The values computed in this manner at the scalar level are plotted for four different time levels as a function of Δ in figure 5. From this figure, a few observations can be made with regard to the behavior of the coefficient.

The coefficient shows the expected behavior for the different resolution levels – it is large for coarser meshes and decreases as the mesh is refined. At very coarse grid levels, the value approaches unity, indicating that the integral length scale expression used in RANS models might be recovered in this limit. In the fine mesh limit, the value seems show a converging behavior also. The behavior of the coefficient is only of interest in as mush as its effect on the eddy viscosity. The eddy viscosity obtained through the use of this grid dependent coefficient should be consistent with the "expected" value obtained from the distribution of ν_s. A plot of the eddy viscosity distribution computed using equation (9) (incorporating the coefficients computed as above) is shown in figure 6.This behavior is compared with the behavior of ν_s seen in figure 4 – it is seen that the behavior of the two functions is qualitatively very similar. Even the quantitative values are in close agreement with each other.

The variable model coefficient can be thought of as a correction to the length scale computed using equation (8). The product $lC_v^*(l/\Delta)$ can be thought of as an effective length scale that provides the correct estimate of the eddy viscosity required to accurately model the unresolved turbulent stresses at any resolution. This has similarities with the dynamic subgrid scale modeling approach where the coefficient is computed dynamically from the resolved scale field. However, in a hybrid approach since the resolution required to mimic such a method cannot always be guaranteed, the coefficient has to be computed a priori.

As originally mentioned, the one equation model has been shown to perform very well for the flows of interest. Therefore, any hybrid approach should recover the LES model in the fine resolution limit. To study the behavior of the eddy viscosity in the LES limit using the coefficient obtained as above, the eddy viscosity computed from equation (9) was correlated with the values predicted by the LES model (equation (6)). This comparison is shown in the form of a correlation coefficient in figure 7. The correlation is seen to be fairly good at all the levels. Keeping in mind that most LES models correlate with DNS data only around the 50% level, this result is extremely good in comparison. As required by the argument presented earlier, the correlation coefficient is seen to approach unity in the limit of fine resolution indicating that the model is able reproduce the SGS eddy viscosity in the fine mesh limit. The reduction in the correlation on the coarse meshes is to be expected because the performance of the LES model at these coarse resolutions is expected to be poor (recall that the correlations at the 32^3 level was only around 48% for the LES model).

CONCLUSION

An approach to combine LES and RANS methodologies to handle practical problems using a length scale model is studied. Testing of the LES model shows that the model correlates very well with DNS results. Examination of the length scale model shows that a variable grid dependent coefficient for the eddy viscosity model is necessary. However, the coefficient computed to do this shows very good behavior in the fine resolution limit. The LES eddy viscosity is reproduced and the coefficient shows an asymptotic behavior in this limit. Its behavior at the low resolution limits reproduces an integral length scale based eddy viscosity. In conclusion, this model shows potential for use in a hybrid approach.

ACKNOWLEDGEMENTS

This work was performed under a Phase II SBIR, Contract No. N68335-98-C-0226, with Naval Air Warfare Center Weapons Division, Technical Monitor: Dr. David Findlay. Computational support for this effort was

provided through the NASA Ames Numerical Aerodynamic Simulator computer complex.

REFERENCES

[1] Sinha, N, York, B.J., Dash, S.M., Chidambaram, N., "A perspective on the simulation of cavity aeroacoustics," AIAA paper 98-0286, 1998.

[2] Speziale, C.G., "Turbulence Modeling for Time-Dependent RANS and VLES: A Review," *AIAA J.*, Vol. 36, No. 2., p 173, February 1998.

[3] Dash, S.M., Perrell, E.R., Kenzakowski, D.C., and Chidambaram, N., "Turbulent Effects on Missile Lateral Control/Divert Jet Interactions," AIAA-99-0809, 37th AIAA Aerospace Sciences Meeting and Exhibit, Reno, NV, January 11–14, 1999.

[4] Clark, R.A., Ferziger, R.A., and Reynolds, W.C., "Evaluation of Subgrid Scale Models using an Accurately Simulated Turbulent Flow," *J. Fluid Mech.*, Vol. 91, pp. 1-16, 1976.

[5] Smagorinsky, J., "General circulation experiments with the primitive equations," *Month. Weath. Rev.*, Vol. 93, 1963, pp. 99-165.

[6] Menon, S., and Kim, W-W., "High Reynolds Number Flow Simulation Using the Localized Dynamic Subgrid Scale Model," AIAA paper No.96-0425, 1996.

[7] Smith, B.R., "The k-kl turbulence model and wall layer model for compressible flows," AIAA paper No. 90-1483.

[8] Comte-Bellot, G., and Corrsin, S., "Simple Eulerian time correlations of full and narrow band velocity signals in grid generated, isotropic turbulence," *J. Fluid Mech.*, Vol 48, 1971, pp 273-337.

[9] Nelson, C.C., "Simulations of spatially evolving compressible turbulence using a local dynamic subgrid model," Ph.D. Thesis, Georgia Institute of Technology, 1997.

[10] Gottleib, D., and Turkel, E., "Dissipative two-four methods for time dependent problems," Mathematics of Computation, Vol. 30 n136, 1976, pp. 703-723.

[11] Ghosal, S., Lund, T.S., Moin, P., and Akselvoll, K., "A dynamic localization model for large eddy simulation of turbulent flows," *J. Fluid Mech.*, Vol. 286, 1995, pp. 229-255.

[12] Erlebacher, G., Hussaini, M.Y., Speziale, C.G., and Zang, T.A., "Toward large eddy simulations of compressible turbulent flows," *J. Fluid Mech.*, Vol. 238, 1992, pp. 155-185.

[13] Mellor, G.L., and Herring, H.J., "A survey of mean turbulent field closure models," *AIAA J.*, Vol. 11, 1973, pp. 590-599.

[14] Kolmogorov, A.N., "The equations of turbulent motion in an incompressible fluid," *Physics,* Vol. 6, No. 1, 1942, pp56-58.

[15] Rotta, J.C., "Statistische Theorie Nichthomogener Turbulenz," *Zeitschrift fur Physik,* Vol. 129, 1951, pp. 547-572.

[16] Wolfshtein, M., "On the length-scale-of-turbulence equation," *Israel J. of Tech.*, Vol. 8, No.1-2, 1970, pp 87-99.

[17] Knight, D., Zhou, G., Okong'o, N., and Shukla, V., "Compressible large eddy simulation using unstructured grids," AIAA paper 98-0535.

[18] Launder, B.E., and Spalding, D.B., "The numerical computation of turbulent flows," *Computational Methods in Applied Mechanical Engineering*, Vol. 3, 1974, pp. 269-289.

[19] Saffman, P.G., "A model for inhomogeneous turbulent flow," *Proc. Roy. Soc. Lond.,* Vol. A317, pp. 417-433.

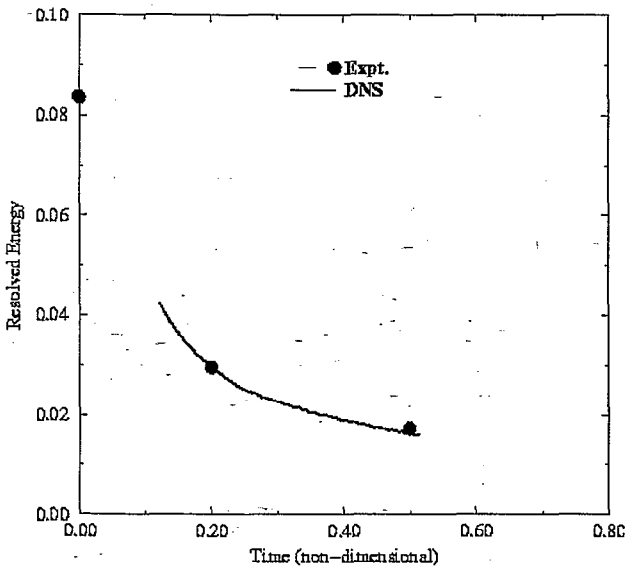

Fig. 1. Comparison of the decay of Turbulent Kinetic Energy obtained from the DNS with experimental data.

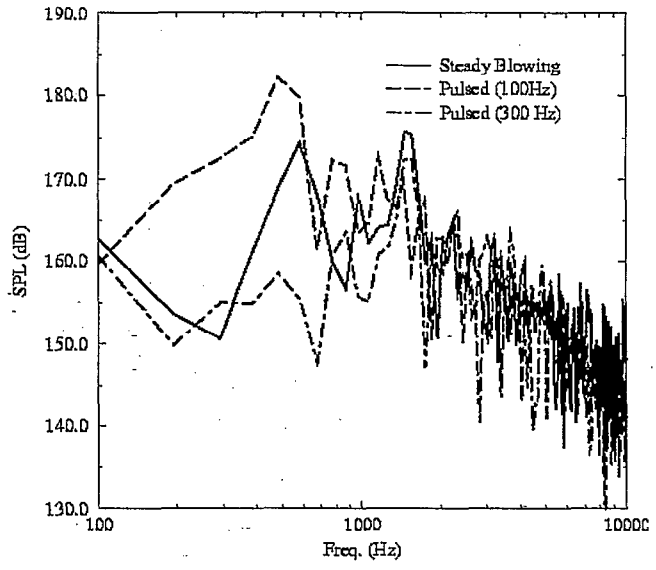

Fig. 3. Spectra of the Sound Pressure Levels at the aft end of the cavity.

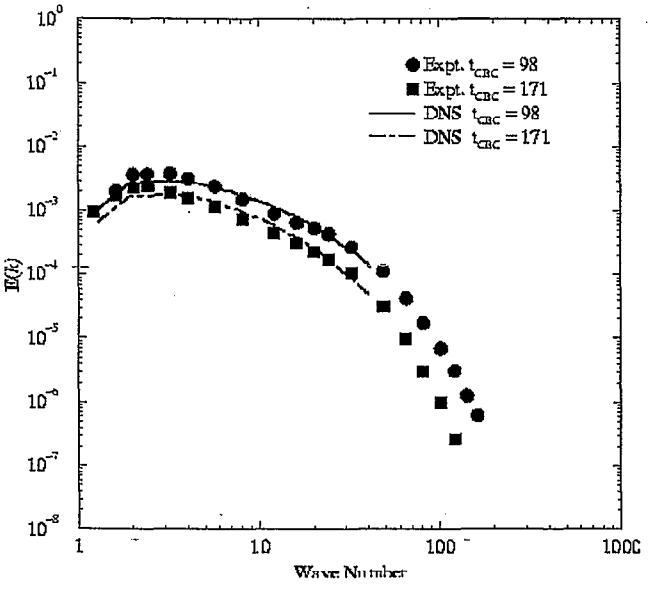

Fig. 2. Comparison of the energy spectra with experimental data.

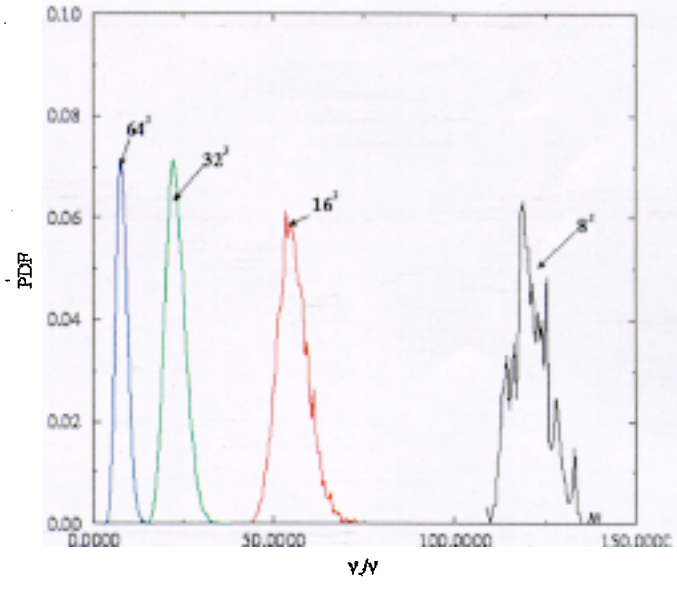

Fig. 4. PDF of ν_s shown for comparison with figure 6. The trends for the ratio of the actual and modeled stresses show a similar form as that for the product $k^{1/2}l$.

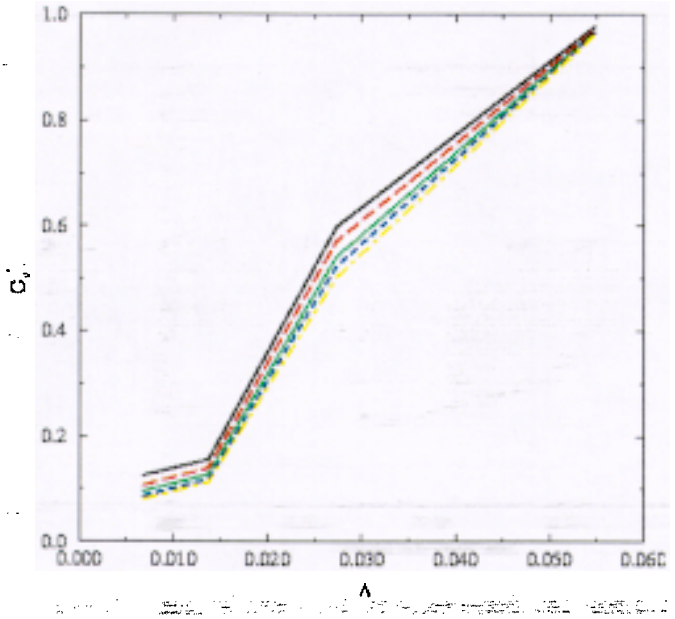

Fig. 5. Plot of the coefficients computed for the *kl* model from the DNS data. The different curves represent different time levels.

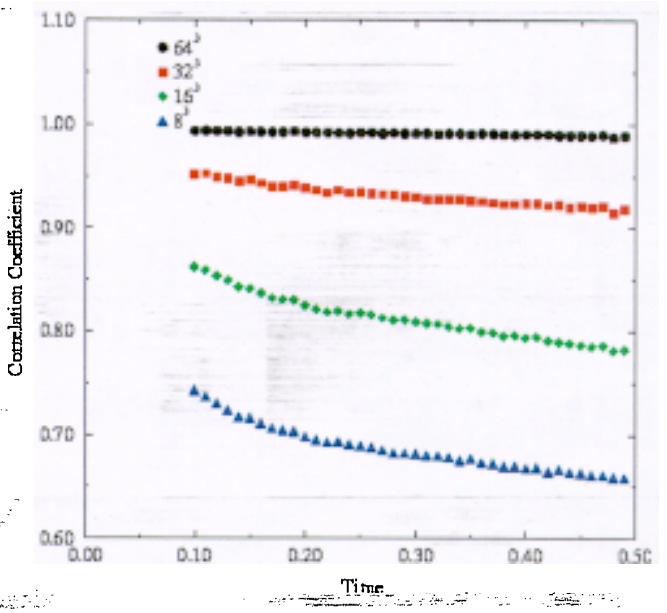

Fig. 7. Correlation between the subgrid eddy viscosity and the eddy viscosity computed from the *kl* model.

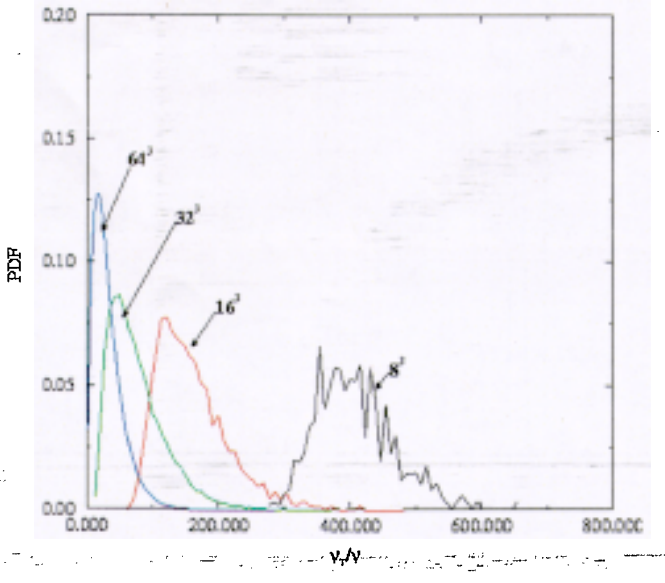

Fig. 6. Plot of the distribution of the eddy viscosity computed using equation (9). The coefficients shown in figure 4 are used at the respective grid levels.